loading combinations which must be investigated by the stress analyst. The envelope is found by eliminating the parameters using any n of the following $n + 1$ equations:

$$\begin{aligned} F(L_1, \ldots, L_n; C_1, \ldots, C_n) &= 0 \\ \partial F/\partial C_1 &= 0 \\ &\cdot \\ &\cdot \\ &\cdot \\ \partial F/\partial C_n &= 0 \end{aligned} \tag{6}$$

Using an exceedance criteria, such as Eq. (5), points on the envelope can be found using numerical approximations of the partial derivatives, then solving simultaneous algebraic equations. The author has used this technique for $n = 2$ and $n = 3$.

Design Load Envelopes for the U_σ Criteria

Using the U_σ design criteria of Eq. (4), and using Eqs. (1) and (2), the parametric equation of the design surface becomes

$$F_{U\sigma}(\Delta L_i, C_i) = (\{C_i\}^T\{\Delta L_i\})^2 - U_\sigma^2\{C_i\}^T[\sigma_{L_{ij}}^2]\{C_i\} = 0$$

which can be written as

$$F_{U\sigma}(\Delta L_i, C_i) = \{C_i\}^T(\{\Delta L_i\}\{\Delta L_i\}^T - U_\sigma^2[\sigma_{L_{ij}}^2])\{C_i\} = 0 \tag{7}$$

so that

$$\left\{\frac{\partial F}{\partial C_i}\right\} = 2(\{\Delta L_i\}\{\Delta L_i\}^T - U_\sigma^2[\sigma_{L_{ij}}^2])\{C_i\} = 0 \tag{8}$$

Substituting,

$$\begin{aligned} \{\bar{C}_i\} &= [Z]\{C_i\} \\ \{\alpha_i\} &= [Z]^{-1}\{\Delta L_i\} \end{aligned} \tag{9}$$

where

$$[Z] = U_\sigma[\sigma_{L_{ij}}^2]^{1/2}$$

($[Z]$ will be real; any of the symmetric square roots may be used.) Equation (8) becomes

$$(\{\alpha_i\}\{\alpha_i\}^T - [I])\{\bar{C}_i\} = 0 \tag{10}$$

Recalling that a matrix formed as the outer product of a vector has only one nonzero eigenvalue, it is seen that Eq. (9) is satisfied if and only if the trace of $\{\alpha_i\}\{\alpha_i\}^T$ equals unity.

Thus, Eq. (9) plus the solution of Eq. (10) give the general solution for design load envelopes satisfying the U_σ criteria.

All points on the design limit surface are given by

$$\{L_i\} = \{L_{\text{mean}_i}\} + U_\sigma[\sigma_{L_{ij}}^2]^{1/2}\{\alpha_i\} \tag{11a}$$

where $\{\alpha_i\}$ are points on the unit n-dimensional sphere

$$\alpha_1^2 + \alpha_2^2 + \ldots + \alpha_n^2 = 1 \tag{11b}$$

and where $[\sigma_{L_{ij}}^2]^{1/2}$ is any of the symmetric square roots of the load covariance matrix. The required matrix square root can be found using standard modal analysis methods.

References

[1] Houbolt, J. C., "Exceedances of Structural Interaction Boundaries for Random Excitation," AFOSR 68-0032, Dec. 1967, Air Force Office of Scientific Research, Arlington, Va.

[2] Hoblit, F. M. et al., "Development of a Power-Spectral Gust Design Procedure for Civil Aircraft," ADS-53, Jan. 1966, Federal Aviation Agency.

Distribution of Lengths of High-Altitude Clear Air Turbulent Regions

EDWARD V. ASHBURN*
Lockheed-California Company, Burbank, Calif.

CROOKS et al.[1] used the results of the analysis of high-altitude clear air turbulence (HICAT) flights 39–175 to determine some measures of the size of HICAT regions. The analysis of the latest series of HICAT flights (flights 180–285) have now been published.[2] In this Note, these new data have been combined with the older data to provide the basis for a determination of the distribution of lengths of HICAT regions. The results of this work are displayed in Fig. 1.

A total of 704 samples for which the flight path was level and the turbulence was indicated to be greater than very light were used to determine the distribution of lengths of the turbulent regions. The percentages of exceedances are given for the total sample, for cases of moderate or greater turbulence (144 cases), for severe turbulence (16 cases), and for those cases for which power spectra and time histories were computed. Time histories and power spectra were computed for only those cases where there was no obvious malfunction of the instruments and the length of the sample was adequate for a power spectra analysis.

The usefulness and the interpretation of the results presented in Fig. 1 depend, to a significant degree, upon the definitions of a turbulent region that were used in preparing the Test Summary Tables of Refs. 1 and 2. The definitions given by Crooks[1] are paraphrased as follows. The selection of clear air turbulence samples was based upon an edit of the flight measurements recorded upon a "quick-look" oscillogram. Turbulence samples were selected primarily from an evaluation of the c.g. normal acceleration response of the aircraft. If continuous rapid c.g. acceleration disturbances in excess of $\pm 0.05\ g$ were observed, turbulence was considered to be present. A turbulent region thus defined was considered to be significant (i.e., the data worth processing) if frequent c.g. acceleration peaks of $\pm 0.10\ g$ or more were observed. In this event, sample (called run and given a number) start and stop times were noted to the nearest 5 sec. Samples of less than 10-sec duration were ignored. Each edited sample was also placed into one of the following categories as shown in Table 1. These criteria were used for sample selection only. The correlation between these criteria and computed gust velocity is good but not perfect.

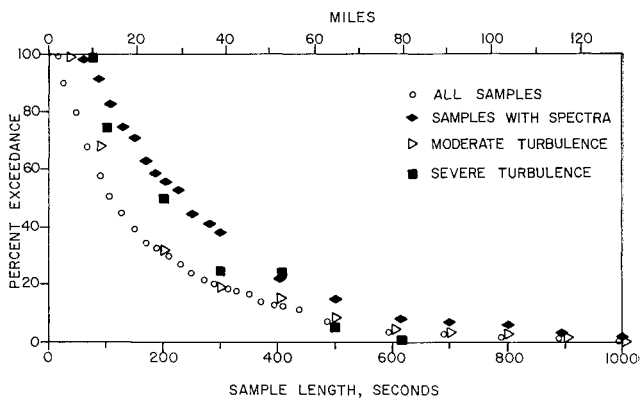

Fig. 1 Percent exceedances of horizontal lengths of high-altitude clear air turbulent regions.

Received May 5, 1969. This work supported under Air Force Flight Dynamics Laboratory, Wright-Patterson Air Force Base, Ohio, under Contract AF-F33615-69-C-1033.

* Head, Atmospheric Physics Laboratory, Rye Canyon Research Center. Member AIAA.

Table 1 Definition of intensity of turbulence

Frequently occurring peak g increment	Descriptive term
±0.05–±0.10	very light
±0.10–±0.25	light
±0.25–±0.50	moderate
±0.50–±0.75	severe
±0.75 or greater	extreme

It is obvious from the definitions given in the previous paragraph that the subjective element in the selection of turbulence samples was not negligible. Subjective judgment was used to determine, for example, if the oscillogram traces indicated one long turbulent region or two or more closely spaced turbulent regions. Throughout the HICAT program more than one person edited the oscillogram records. Even though a strong effort was made to obtain uniformity in judgment, individual differences in judgment probably were not eliminated. In addition, changes in judgment on the length of a run undoubtedly occurred as individual experience was gained. A relatively high number of samples at the even 4, 6, 7, and 10 min indicates some personal bias. An arbitrary upper limit of 1000 sec was established because of the data processing computer program. Thus, the statistical information presented in Fig. 1 is biased because of the elimination of the very short and the very long turbulent regions; because the pilot, in a few cases, turned the aircraft before completely penetrating the turbulent regions and because the criteria for the intensity of turbulence do not include the gust velocities. On the whole, however, the results presented in Fig. 1 probably provide an adequate representation of the relative frequencies of occurrence of the turbulent regions whose length are in the intermediate range.

Further measurements and analysis are required to answer relevant questions such as 1) What are the horizontal shapes of the turbulent regions? 2) How do the shapes and lengths change in time with respect to axis fixed to the earth and with respect to axis fixed to a volume element of the atmosphere?

References

[1] Crooks, W. M. et al., "Project HICAT An Investigation of High Altitude Clear Air Turbulence," TR AFFDL-TR-67-123, Nov. 1967, Lockheed-California Co., Burbank, Calif.

[2] Crooks, W. M. et al., "Project HICAT High Altitude Lear Air Turbulence Measurements and Meteorological Correlations," TR AFFDL-TR-68-127, Nov. 1968, Lockheed-California Co., Burbank, Calif.

An Algorithm for the Induced Velocity of Curved Vortex Lines

THOMAS ARTHUR MCMAHON*
Massachusetts Institute of Technology, Cambridge, Mass.

Nomenclature

Ψ = stream function
Γ = circulation about vortex ring, vortex line
V_z = normal component of induced velocity
R = vortex ring radius
r,z = field point coordinates (dimensional)
θ_i,θ_r = angles of incidence and reflection of hypothetical rays
x = dimensionless radial distance, r/R
∂ = dimensionless axial distance, z/R

Received February 28, 1969.
* Research Assistant.

Introduction

MANY problems in aerodynamics, such as propeller theory and rotary wind theory, involve calculating the induced velocity due to curved vortex lines. Provided one knows the geometry of such lines, the induced velocity at any point may be calculated by the Biot-Savart law. Occasionally it is useful to have a scheme for approximating the line integration this law requires. Such a scheme is advanced here.

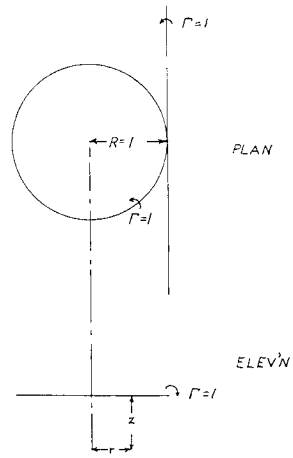

Fig. 1 Coordinate system

Proposing the Algorithm

Consider the geometry of Fig. 1, which represents a vortex ring and a tangent vortex line of equal strength. It is proposed to calculate the normal component of induced velocity due to the ring in any plane parallel to the plane of the ring and displaced a height z, and to compare it with that appropriate for the vortex line. The stream function at a point P in the flowfield of a vortex ring of strength Γ and radius R is given in Ref. 2 as

$$\Psi = -(\Gamma R/2)(d_1 + d_2)[K(\tau) - E(\tau)] \quad (1)$$

where Rd_1 and Rd_2 are the least and greatest distances of the point P to the vortex ring,

$$\tau = (d_2 - d_1)/(d_2 + d_1) \quad (2)$$

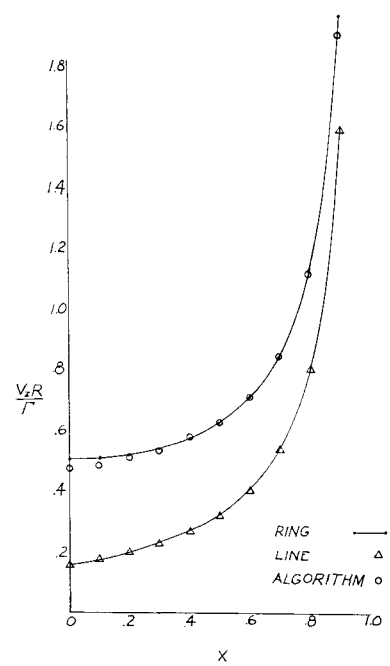

Fig. 2. Induced velocity comparison, $\partial = z/R = 0$.